G-protein signaling modulator 1 deficiency accelerates cystic disease in an orthologous mouse model of autosomal dominant polycystic kidney disease

Michelle Kwon[a,1], Tengis S. Pavlov[b,1], Kandai Nozu[c], Shauna A. Rasmussen[b], Daria V. Ilatovskaya[b], Alexandra Lerch-Gaggl[d], Lauren M. North[a], Hyunho Kim[e,2], Feng Qian[e,2], William E. Sweeney, Jr.[c], Ellis D. Avner[b,c], Joe B. Blumer[f], Alexander Staruschenko[b], and Frank Park[a,b,3]

[a]Division of Nephrology, Department of Medicine, and Departments of [b]Physiology, [c]Pediatrics, and [d]Pathology, Medical College of Wisconsin, Milwaukee, WI 53226; [e]Division of Nephrology, Department of Medicine, The Johns Hopkins University School of Medicine, Baltimore, MD 21205; and [f]Department of Cell and Molecular Pharmacology, Medical University of South Carolina, Charleston, SC 29425

Edited by Marilyn G. Farquhar, University of California at San Diego, La Jolla, CA, and approved November 13, 2012 (received for review October 2, 2012)

Polycystic kidney diseases are the most common genetic diseases that affect the kidney. There remains a paucity of information regarding mechanisms by which G proteins are regulated in the context of polycystic kidney disease to promote abnormal epithelial cell expansion and cystogenesis. In this study, we describe a functional role for the accessory protein, G-protein signaling modulator 1 (GPSM1), also known as activator of G-protein signaling 3, to act as a modulator of cyst progression in an orthologous mouse model of autosomal dominant polycystic kidney disease (ADPKD). A complete loss of *Gpsm1* in the *Pkd1*$^{V/V}$ mouse model of ADPKD, which displays a hypomorphic phenotype of polycystin-1, demonstrated increased cyst progression and reduced renal function compared with age-matched cystic *Gpsm1*$^{+/+}$ and *Gpsm1*$^{+/-}$ mice. Electrophysiological studies identified a role by which GPSM1 increased heteromeric polycystin-1/polycystin-2 ion channel activity via Gβγ subunits. In summary, the present study demonstrates an important role for GPSM1 in controlling the dynamics of cyst progression in an orthologous mouse model of ADPKD and presents a therapeutic target for drug development in the treatment of this costly disease.

accessory proteins | renal epithelial cells | patch clamp | renal injury | heterotrimeric G protein

Polycystic kidney disease (PKD) is a common monogenetic cause of chronic renal failure in children and adults. Positional cloning has identified the genes responsible for the etiology of PKD, with mutations in *PKD1* (1, 2) and *PKD2* (3) being associated with the dominant form of this disease. The hallmark phenotype in PKD is the manifestation of fluid-filled renal cysts, which originate from the expansion of de-differentiated and actively proliferating tubular epithelia (4). Abnormalities in gene expression, cell polarity, fluid secretion, apoptosis, and extracellular matrix have been shown to play key roles in the pathogenesis of PKD (5, 6).

Heterotrimeric G proteins (or G proteins) are pivotal signaling integrators that facilitate the transmission of information from the external milieu to the intracellular compartment. Classically, G-protein activation involves hormonal or mechanical stimulation of cell-surface G-protein–coupled receptors (GPCR). Polycystin-1 (PC1) is believed to act as an atypical GPCR at the cell surface of renal epithelial cells to directly control the function of the polycystin-2 (PC2) ion channel (7, 8), in addition to controlling the activity of specific G-protein subunits (9–13). Among its many cellular sites, PC2 localizes to the ciliary membrane and acts as a mechanosensor (14). Recently, a number of therapeutic drugs targeting GPCR to reduce cyst progression have reached the clinical trial stage, validating a central role for G proteins in cystic disease pathogenesis (5).

Over the past 15 years, our basic understanding regarding the interaction between GPCR, G proteins, and their subsequent effector has become more diverse, largely due to the discovery of accessory proteins that regulate the G-protein activation/inactivation cycle through a GPCR-independent pathway (15, 16). One group of accessory proteins known as activator of G-protein signaling (AGS) proteins were identified as GPCR-independent regulators of G-protein subunits (15, 16). In particular, G-protein signaling modulator 1 (GPSM1), also known as activator of G-protein signaling 3 (AGS3), was identified as an evolutionarily conserved protein with orthologs also found in fruit flies and worms (17, 18). GPSM1 contains four G-protein regulatory (GPR) motifs, also known as GoLoco motifs (18, 19), which function as a guanine nucleotide dissociation inhibitor (GDI) (18, 20).

In nonrenal mammalian cells and whole-organ systems, GPSM1 plays a critical role in regulating mitotic spindle orientation, cell polarity, and adenylyl cyclase activity (15, 21, 22). Similar biological properties have been attributed to GPSM1 orthologs in invertebrates (15, 21, 22). These same biological processes have been identified as central pathophysiological mechanisms promoting cystogenesis in PKD, but the role of GPSM1 in the kidney remains undefined. Recently, our laboratory has identified an abnormally high expression level of GPSM1 in renal epithelial cells obtained from multiple models of PKD (23) and in noncystic kidneys following renal injury (24). In the latter model, the deficiency in the expression of GPSM1 following acute kidney injury resulted in impaired recovery of the sublethally injured tubular epithelial cells (24). This set of data suggests that GPSM1 plays a role in renal epithelial cell repair following renal injury and that the induction of this protein in PKD may be a critical modulator of the renal cystogenic process.

The present study was designed to investigate the role of GPSM1 in renal epithelial cell cystogenesis using an orthologous mouse model of autosomal dominant polycystic kidney disease (ADPKD). *Gpsm1* null mice were intercrossed with a mouse model of ADPKD, *Pkd1*$^{V/V}$, which exhibits wild-type PC1 hypomorphism, to provide genetic insight into the role of GPSM1 in PKD biology.

Results

Expression and Localization of GPSM1 Protein in a Mouse Model of ADPKD. The expression profile and segment-specific localization of *GPSM1* was examined using kidneys from an orthologous PC1 hypomorphic mouse model, *Pkd1*$^{V/V}$, previously described

Author contributions: T.S.P., A.L.-G., A.S., and F.P. designed research; M.K., T.S.P., K.N., S.A.R., D.V.I., A.L.-G., L.M.N., A.S., and F.P. performed research; H.K., F.Q., W.E.S., E.D.A., and J.B.B. contributed new reagents/analytic tools; M.K., T.S.P., K.N., S.A.R., D.V.I., A.L.-G., W.E.S., J.B.B., A.S., and F.P. analyzed data; and J.B.B., A.S., and F.P. wrote the paper.

The authors declare no conflict of interest.

This article is a PNAS Direct Submission.

[1]M.K. and T.S.P. contributed equally to this work.

[2]Present address: University of Maryland School of Medicine, Medicine/Nephrology, Baltimore, MD 21201.

[3]To whom correspondence should be addressed. E-mail: fpark@mcw.edu.

This article contains supporting information online at www.pnas.org/lookup/suppl/doi:10.1073/pnas.1216830110/-/DCSupplemental.

by Yu et al. (25). GPSM1 protein expression by immunoblot analysis is shown between normal and cystic mouse kidneys of various genotypes at postnatal day 11–12 (P11–12) (Fig. 1*A*). Quantitation of the GPSM1 band intensities revealed that cystic $Gpsm1^{+/+};Pkd1^{V/V}$ kidneys expressed significantly higher levels of GPSM1 protein by ~15-fold ($P < 0.001$) compared with age-matched noncystic $Gpsm1^{+/+};Pkd1^{+/+}$ mouse kidneys (Fig. 1*B*). Similarly, renal GPSM1 protein is readily detectable in cystic $Pkd1^{V/V}$ kidneys at P19, and the expression was directly correlated with the *Gpsm1* genotype (Fig. S2*A*). Using another model of ADPKD (26), we observed that GPSM1 levels remained elevated in the cystic kidneys beyond P14 at which time normal C57BL/6 mice (i.e., $Gpsm1^{+/+};Pkd1^{+/+}$) appear to have low-to-undetectable levels of expression (Fig. S1). The virtually undetectable expression of GPSM1 in older wild-type kidneys in our study is in agreement with previously published reports using mature kidneys from mice, rats, and humans (23, 24, 27, 28). Moreover, the temporal renal GPSM1 expression profile is similar to previous studies using brain samples (27, 29).

Immunofluorescent histochemistry of serial renal sections from $Gpsm1^{+/+};Pkd1^{V/V}$ at P12 demonstrated that GPSM1 protein expression was predominantly localized to the cystic epithelial cells of collecting duct origin [Dolichol biflorus agglutinin (DBA)–positive cells in red in Fig. 2]. In agreement with the original description of this *Pkd1* model (25), renal cysts in $Pkd1^{V/V}$ mice are predominantly derived from collecting ducts (DBA-positive in red) with a small number of cysts in distal tubules (Calbindin 28K-positive in red) and proximal tubules [Lotus tetragonobulus agglutinin (LTA)-positive in brown] (Fig. S3*A*). These results confirm the previous study by Yu et al. (25) describing this ADPKD mouse model.

Complete Loss of Renal GPSM1 Increases Cystogenesis in $Pkd1^{V/V}$ Mice. Double heterozygous $Gpsm1^{+/-};Pkd1^{V/+}$ breeder mice were produced as described in *SI Materials and Methods* and intercrossed to generate a panel of mice with various combinations of *Gpsm1;Pkd1* genotypes. The gross morphology of representative P11–12 whole kidneys from noncystic ($Pkd1^{+/+}$ and $Pkd1^{+/-}$) and cystic $Pkd1^{V/V}$ mice with each *Gpsm1* genotype ($^{+/+}$, $^{+/-}$, and $^{-/-}$) were compared to determine genotype–phenotype correlations (Fig. 3*A*).

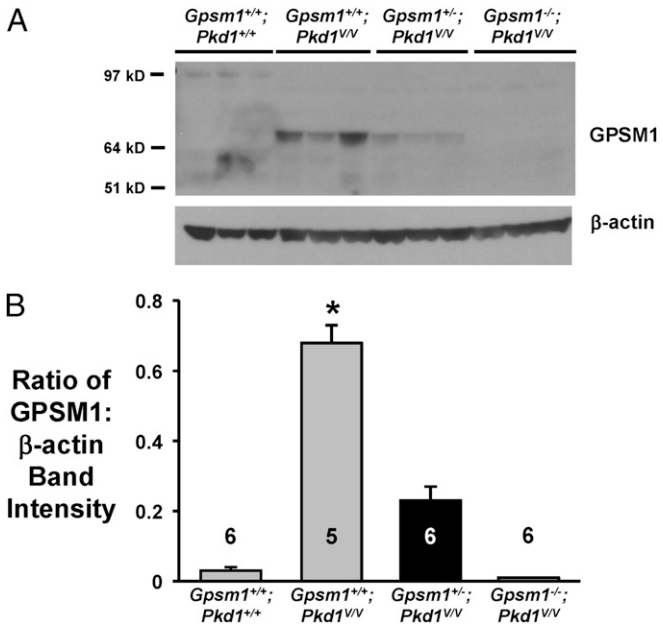

Fig. 1. GPSM1 protein expression profile in various *Gpsm1;Pkd1* genotyped mice. Mouse kidneys were harvested between postnatal days 11 and 12 from noncystic $Gpsm1^{+/+};Pkd1^{+/+}$ and cystic $Pkd1^{V/V}$ mice with various *Gpsm1* genotypes (i.e., $Gpsm1^{+/+}$, $Gpsm1^{+/-}$, or $Gpsm1^{-/-}$). (*A*) Whole-kidney protein lysates were analyzed for the expression of GPSM1 using immunoblot analysis ($n = 5$–6 samples/genotype). β-Actin was used as a loading control. (*B*) Densitometric analysis of the band intensity of GPSM1 relative to the loading control (β-actin). *$P < 0.001$ indicates significant differences among all other groups. The number of animals examined is shown in each bar.

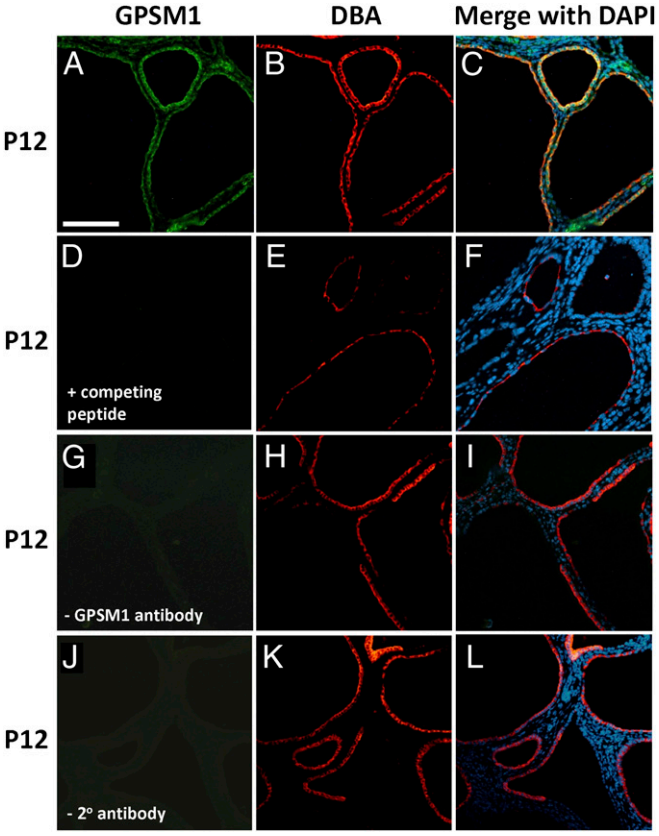

Fig. 2. GPSM1 localization in cystic ADPKD mouse kidneys by immunofluorescent histochemistry. Serial sections were made from kidneys harvested at postnatal day 12 from cystic $Gpsm1^{+/+};Pkd1^{V/V}$ mice. Kidney sections were stained with GPSM1 (green color in *A*) and a collecting duct lectin (DBA; red color in *B*, *E*, *H*, and *K*). Nuclei were stained with DAPI (blue color in *C*, *F*, *I*, and *L*). Negative controls for GPSM1 staining were sections incubated with competing peptide (*D*), no primary GPSM1 antibody (*G*), and no secondary antibody (*J*). Magnification 40×. (Scale bar: 0.1 mm for all images.)

Kidney-to-body weight (KW/BW) ratios provide a reliable index of renal cystogenesis in animal models of PKD. Using this parameter, the KW/BW ratios at P11–12 for $Pkd1^{V/V}$ mice were significantly higher ($P < 0.001$) regardless of the *Gpsm1* genotype compared with the wild-type mice ($Gpsm1^{+/+};Pkd1^{+/+}$) (Fig. 3*B*). The KW/BW ratio for $Gpsm1^{-/-};Pkd1^{V/V}$ mice was 19.4 ± 4.3% ($n = 7$), which was significantly higher ($P < 0.05$) by 85% (10.5 ± 0.6%; $n = 11$) in $Gpsm1^{+/-};Pkd1^{V/V}$ and by 54% (12.6 ± 2.7%; $n = 8$) in $Gpsm1^{+/+};Pkd1^{V/V}$ mouse kidneys. There was no difference in KW/BW ratios between all of the noncystic $Pkd1^{+/+}$ or $Pkd1^{+/V}$ mouse kidney groups regardless of the *Gpsm1* genotypes (Fig. 3*B*).

Whole-kidney sections were obtained from the middle of the several different kidneys from $Pkd1^{V/V}$ mice with either wild-type $Gpsm1^{+/+}$, heterozygous $Gpsm1^{+/-}$, or null $Gpsm1^{-/-}$ (Fig. 3*C*). The percentage of total surface area composed of cystic space or renal parenchyma was assessed by quantitative morphometry (Fig. 3*D*). Cystic $Pkd1^{V/V}$ mice with either heterozygous ($Gpsm1^{+/-}$) or wild-type ($Gpsm1^{+/+}$) expression had significantly greater amounts of parenchymal surface area by 32% (36.2 ± 2.0%; $P < 0.05$; $n = 11$) and by 23% (33.5 ± 2.3%; $P < 0.05$; $n = 7$) compared

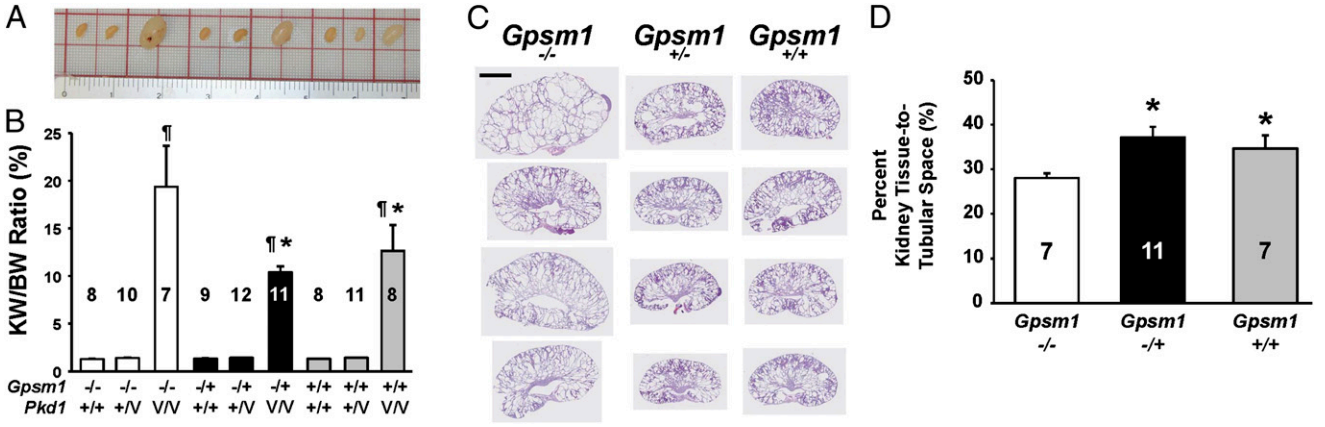

Fig. 3. Biological analysis of the renal cystic index in various *Gpsm1;Pkd1* genotyped mice. Mouse kidneys were harvested between postnatal days 11 and 12 from noncystic $Pkd1^{+/+}$ and $Pkd1^{+/V}$ and cystic $Pkd1^{V/V}$ mice with various *Gpsm1* genotypes (i.e., $Gpsm1^{+/+}$, $Gpsm1^{+/-}$, or $Gpsm1^{-/-}$). (*A*) Representative whole kidneys were photographed to demonstrate the differences in gross morphology among the various genotyped mice. (*B*) KW/BW ratios were calculated and graphed as a percentage. Numbers analyzed for each group with a distinct genotype are provided in the graph. $*P < 0.05$: significant difference between $Gpsm1^{+/+};Pkd1^{V/V}$ and $Gpsm1^{+/-};Pkd1^{V/V}$ versus $Gpsm1^{-/-};Pkd1^{V/V}$. $¶P < 0.001$: significant difference between the $Pkd1^{V/V}$ versus $Pkd1^{+/+}$ and $Pkd1^{+/-}$ mouse kidneys. (*C*) Kidneys obtained from mice at postnatal days 11–12 as shown in *A* were sectioned and stained with H&E. Four representative whole-kidney sections are shown from the three different *Gpsm1* genotyped mouse strains on the $Pkd1^{V/V}$ background. (Scale bar: 2.98 mm.) Kidney sections were morphometrically analyzed as described in *Materials and Methods* and graphed in *D* to determine the surface area of the remaining kidney tissue relative to the tubular (cyst) space. $*P < 0.05$: significant difference between $Gpsm1^{+/+};Pkd1^{V/V}$ and $Gpsm1^{+/-};Pkd1^{V/V}$ versus $Gpsm1^{-/-};Pkd1^{V/V}$ mouse kidneys.

with null GPSM1-expressing $Pkd1^{V/V}$ mice ($Gpsm1^{-/-}$; 27.1 ± 1.7%; $n = 7$).

Proliferating cell nuclear antigen-positive renal cystic epithelial cells were significantly higher ($P < 0.05$) in $Gpsm1^{-/-};Pkd1^{V/V}$ compared with $Gpsm1^{+/+};Pkd1^{V/V}$ mouse kidneys (Fig. S3*C*). Neither the extent of renal fibrosis as determined by Trichrome staining (Fig. S3*B*) nor the level of α-smooth muscle actin staining in the kidney was markedly different between cystic kidneys with or without the expression of GPSM1 (Fig. S3*D*). Macrophage infiltration into the kidney was absent as determined by a lack of F4/80-positive cells in the cystic kidneys (data not shown). At P19, there was a similar trend as observed at P11–12 where the KW/BW ratio (Fig. S2*B*) and morphometric tissue-to-tubular space analysis (Fig. S2*C*) were elevated in the absence of *Gpsm1* compared with the mice expressing *Gpsm1* ($^{+/+}$ or $^{+/-}$) in the $Pkd1^{V/V}$ mice.

Reduction of Renal Function in $Pkd1^{V/V}$ Mice with a Genetic Loss in *Gpsm1*. To assess the level of renal function in the normal and cystic mice, blood urea nitrogen (BUN) (Fig. 4*A*) and plasma creatinine (Fig. 4*B*) were measured at P11-12, and BUN was measured at P19 (Fig. S2*I*). In Fig. 4*A*, the BUN was not different between $Pkd1^{+/+}$ mice with or without a functional *Gpsm1* gene. BUN was significantly higher ($P < 0.001$ to $P < 0.05$) in all of the $Pkd^{V/V}$ mice regardless of *Gpsm1* genotype compared with the $Pkd1^{+/+}$ mice. However, the BUN levels increased with a complete loss of the *Gpsm1* genes, such that BUN was significantly higher in the $Gpsm1^{-/-};Pkd1^{V/V}$ mice ($n = 7$) compared with $Gpsm1^{-/+};Pkd1^{V/V}$ ($P < 0.01$; $n = 9$) and $Gpsm1^{+/+};Pkd1^{V/V}$ ($P < 0.05$; $n = 5$) mice. Subsequently, plasma creatinine showed a consistent range of 0.10–0.13 mg creatinine/dL (average = 0.11 ± 0.01 mg/dL; $n = 8$) in noncystic $Gpsm1^{-/-};Pkd1^{+/+}$ mice (Fig. 4*B*). Consistent with the BUN results, the trend of the plasma creatinine levels was highest in the mice with a complete loss of the *Gpsm1* gene. Plasma creatinine was 0.194 ± 0.022 mg/dL ($n = 5$) in the $Gpsm1^{-/-};Pkd1^{V/V}$ mice, which was 49% ($P < 0.01$; $n = 11$) and 24% ($n = 5$) higher than the levels detected in the $Gpsm1^{+/-};Pkd1^{V/V}$ (0.13 ± 0.01 mg/dL) and $Gpsm1^{+/+};Pkd1^{V/V}$ (0.156 ± 0.01 mg/dL) mice, respectively. The reduced renal function in each of the mouse groups was consistent with the increased KW/BW ratios (Fig. 3*B*) and the decreased tissue surface area (Fig. 3*D*).

To assess whether there may have been a prerenal effect, such as volume status and dehydration, in the $Pkd1^{V/V}$ mice, we measured the plasma Na^+ and K^+ levels in each of the mouse groups at P19 (Fig. S2 *D* and *E*). No difference was measured between the noncystic and cystic mice. Cyst fluid analysis similarly did not detect differences in the Na^+ and K^+ levels nor in osmolality regardless of the *Gpsm1* genotype (Fig. S2 *F–H*).

Electrophysiological Studies Demonstrating Increased PC1/PC2 Channel Activity in the Presence of GPSM1. The expression of PC1 and PC2 leads to a physical interaction between PC1 and PC2 (7, 8, 30–33) to form a Ca^{2+}-permeable nonselective cation channel (10, 34, 35). Fig. 5 demonstrates that GPSM1 modulates PC1/PC2 channel activity. PC1/PC2 channel activity was measured

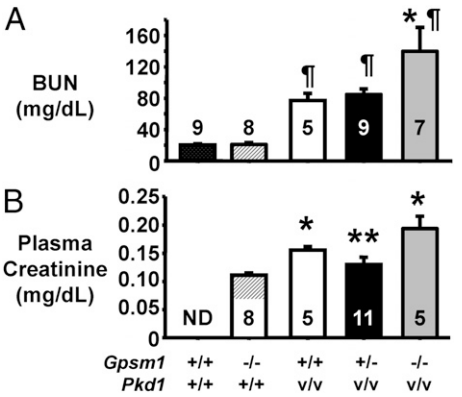

Fig. 4. Decreased renal function in $Pkd1^{V/V}$ mice with *Gpsm1* gene deficiency. Plasma was obtained from mice between P11 and P12 to measure the levels of either BUN (*A*) or creatinine (*B*) as a measure of renal function. (*A*) $*P < 0.05$ to $P < 0.01$: significant difference between $Gpsm1^{-/-};Pkd1^{V/V}$ and the other two $Pkd1^{V/V}$ mouse groups. $¶P < 0.05$ to $P < 0.001$: higher significant difference between all $Pkd1^{V/V}$ groups and both $Pkd1^{+/+}$ groups. (*B*) $*P < 0.05$: significant difference between noncystic $Gpsm1^{-/-};Pkd1^{+/+}$ mice and the $Pkd1^{V/V}$ groups. $**P < 0.01$: significant difference between $Gpsm1^{+/-};Pkd1^{V/V}$ and $Gpsm1^{-/-};Pkd1^{V/V}$ mice. The numbers for each distinct genotype are shown in the bars of each graph. ND, not determined.

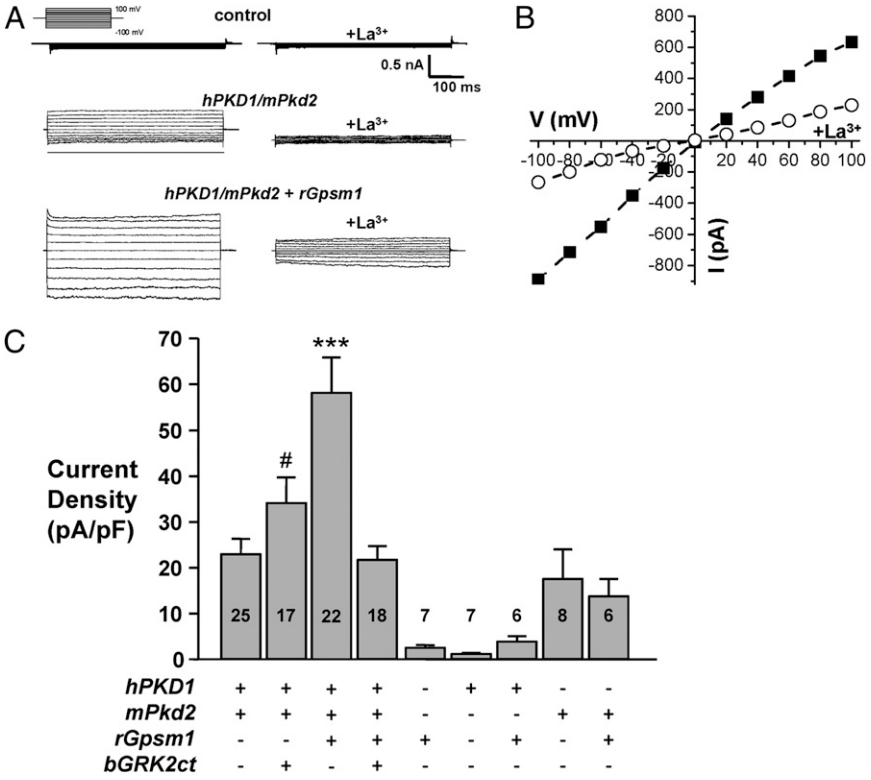

Fig. 5. GPSM1 enhances PC1/PC2 activity. (*A*) Typical macroscopic currents before and after La^{3+} under voltage-clamp conditions from nontransfected (control) CHO cells or transfected with human *PKD1* (2 μg) and mouse *Pkd2* (1 μg) either alone or coexpressed with rat *Gpsm1* (1 μg). Currents were elicited by test pulses with 20-mV steps from 100 to −100 mV from a holding potential of 0 mV. Voltage pulse protocol is shown in the inset. (*B*) Representative macroscopic I/V relation before (closed squares) and after (open circles) La^{3+} from the experiment presented in *A*. (*C*) Summary graph of the La^{3+}-sensitive current at −100 mV for voltage-clamped CHO cells expressing PC1 and PC2 in the absence and presence of wild-type rat GPSM1 (rGpsm1) or bovine GRK2ct (bGRK2ct). The number of observations in each group is shown in each bar. ***$P < 0.001$ versus all groups; $^{\#}P < 0.05$: significant difference between *hPKD1/mPkd2 + rGpsm1* and *hPKD1/mPkd2 + bGRK2ct*.

as the La^{3+}-sensitive inward Na^+ current at −100 mV under voltage-clamp conditions. La^{3+} is a nonselective cation channel inhibitor and has been shown to inhibit PC2 channel activity (34, 35). As shown in Fig. 5*A*, CHO cells did not exhibit endogenous La^{3+}-sensitive currents. Macroscopic currents from representative whole-cell experiments elicited by a family of test pulses stepping from a holding potential of 0 to 100 to −100 mV are shown in the absence and presence of GPSM1 (Fig. 5*B*). Fig. 5*A* shows currents before (left) and following (right) treatment with $LaCl_3$ (1 mM). The current–voltage (I–V) relation for macroscopic PC1/PC2 currents in the presence of GPSM1 is shown in Fig. 5*B*.

As summarized in Fig. 5*C*, electrophysiological analysis of CHO cells transfected with *rGpsm1*- or *hPKD1*-expressing plasmids alone or in combination produced minimal La^{3+}-sensitive currents, which represent basal activity of the endogenous channels in CHO cells. CHO cells transfected with *mPkd2*-expressing plasmid generated ion channel activity, but the overexpression of GPSM1 did not significantly alter the magnitude of the activity. Coexpression of *hPKD1* and *mPkd2* did not significantly alter the ion channel activity compared with the CHO cells expressing *mPkd2* alone. However, coexpression of GPSM1 with PC1/PC2 significantly increased ($P < 0.001$) La^{3+}-sensitive current by 2.5-fold from 23.0 ± 3.3 pA/pF ($n = 25$) to 58.3 ± 7.7 pA/pF ($n = 22$). Blockade of Gβγ function with GRK2ct, a selective Gβγ scavenger, prevented the GPSM1-mediated increase in PC1/PC2 activity (21.7 ± 3.0 pA/pF; $n = 18$) compared with the basal PC1/PC2 channel activity in the presence of GRK2ct (34.1 ± 5.6 pA/pF; $n = 17$).

In pertussis toxin (PTX)-treated CHO cells transfected with *hPKD1/mPkd2* (Fig. S4), the La^{3+}-sensitive ion channel current density was 14.7 ± 3.3 pA/pF ($n = 7$). Upon overexpression of GPSM1, the PC1/PC2 channel activity significantly increased ($P < 0.05$) by 2.4-fold to 33.3 ± 3.4 pA/pF ($n = 12$). As pertussis toxin pretreatment does not inhibit the GPSM1–Gαi interaction (36), these data would further suggest that PC1/PC2 channel activity is regulated by unbound Gβγ dimers liberated by GPSM1.

Discussion

The association between extrinsic cues, including hormones and mechanical forces, with cell-surface GPCRs has long been studied to understand the activation/inactivation states of heterotrimeric G proteins to modulate cell-signaling pathways (5). With the identification of accessory proteins, however, the control of G-protein mediated signaling has become more diverse (16, 37, 38). Accessory proteins are postulated to possess a multitude of intracellular functions, including modulating signal intensity and/or duration, orienting signaling components to specific subcellular locations, and contributing to the formation of functional signaling complexes that regulate the directionality of signaling pathways. One example of such an accessory protein is the group II AGS protein, GPSM1 (16, 37).

At present, there remains a paucity of information regarding the role of accessory proteins, including GPSM1, in the kidney. Our recently published data (23, 24) in combination with the results of our present study are consistent with GPSM1 playing an integral role in modulating mechanisms involved in epithelial cell repair and cyst formation. The morphogenetic changes that cystic epithelial cells follow are similar to those observed during regeneration and repair processes in noncystic renal epithelial cells following an acute insult, such as ischemic injury (39, 40). Following injury, kidneys undergo highly organized and coordinated repair in which epithelial cells undergo partial dedifferentiation, cell migration, and proliferation to reform functional nephrons (41, 42). The role that the polycystins play in this repair process is not fully known, but the expression of *Pkd1* and *Pkd2* mRNA and proteins is increased following ischemia-reperfusion injury (IRI) (43, 44). Moreover, the genetic loss of either one of the *Pkd1* or *Pkd2* genes leads to an impairment in the recovery of the epithelial cell and promotes focal cyst formation following renal injury (45–47). It is entirely possible that kidneys with mutations in either ADPKD gene would have areas of localized ischemia and cell damage due to cystic growth. This would initiate a repair process very similar to the process that occurs following ischemia-reperfusion injury (IRI). As the cysts

expand, the repair process continues to be activated and renal epithelial cells with cystic gene mutations remain in a continual state of repair, leading to cyst expansion and abnormal tissue architecture (39, 40). Because we have shown that mice deficient for full-length GPSM1 expression have a markedly reduced capacity to promote renal epithelial cell recovery following IRI compared with wild-type *Gpsm1*$^{+/+}$ mice (24) and that there is an association with GPSM1 and polycystin ion channel activity (see below), we believe that there may be a close association between GPSM1, polycystins, and pathways involved in epithelial cell repair to modulate cystogenesis in animal models of PKD.

At this time, the mechanism of action for GPSM1 in the renal epithelial cells remains elusive, although several modes of action have been proposed. First, GPSM1 is known to function as a GDI by selectively binding to $G\alpha_{i/o}$ subunits in the GDP state (20, 28, 48). Because $G\alpha_i$ subunits inhibit adenylyl cyclase activity and elevated levels of cAMP is a classic phenotype observed in cystic renal epithelial cells (5), the relationship between GPSM1, $G\alpha_i$, and adenylyl cyclase was initially of particular interest. Numerous clinical trials based on somatostatin receptor agonists, which activate $G\alpha_i$ subunits, are currently being investigated as an anticystic agent in PKD (5). Because a single molecule of GPSM1 can simultaneously bind up to four $G\alpha_i$ subunits (49), it is conceivable that GPSM1 could short-circuit the ability of $G\alpha_i$ subunits to inhibit adenylyl cyclase. Fan et al. (50) demonstrated this phenomenon using cultured neuronal cells by measuring increased activation of cAMP production in the presence of elevated GPSM1 levels. To date, however, our laboratory and others have been unable to show any measurable difference in cAMP production in cultured renal epithelial cells and other nonrenal-derived cells with or without GPSM1 expression (23, 24, 51).

For this reason, we believe that the role of GPSM1 and $G\alpha_i$-mediated signaling is substantially more diverse than previously anticipated (36). The GPR motifs in the C-terminal region of GPSM1 compete with Gβγ for Gαi-GDP binding (36, 52), and therefore part of their mode of action may be to release free Gβγ to mediate their biological function (18, 23, 53, 54). Gβγ was used as the downstream signaling cassette to determine their growth phenotypes in the original yeast-based screen to isolate GPSM1 (17, 18). In mammals, Sanada et al. (54) showed that GPSM1 influences Gβγ subunits to regulate mitotic spindle orientation in the developing rat brain. Moreover, Bowers et al. (53) demonstrated that sequestering Gβγ dimers in the nucleus accumbens blocked ethanol-seeking behavior in rats. Studies have shown that Gβγ dimers can activate downstream mitogen-activated protein kinase pathways (55, 56) or regulate ion channel function (10, 11).

In our study, the GPSM1-Gβγ mediated an increase in the La^{3+}-sensitive PC1/PC2 channel activity. PC2 is a nonselective cation channel (57, 58) in which numerous interacting proteins, including PC1 (8, 9), can bind to regulate its endogenous activity (57, 58). The coexpression of PC1 with PC2 appeared to facilitate the increased activity of the ion channel by GPSM1 because GPSM1 had no discernible effect on PC2 channel activity in the absence of PC1. The role for Gβγ in modulating PC1/PC2 channel activity is consistent with a previous study in neurons by Delmas et al. (10) where the inhibition of PC1/PC2 calcium currents by MR3, a putative ligand for PC1, was blocked in the presence of Gα-transducin, a potent Gβγ-sequestering agent. It may be possible that Gβγ either directly interacts with the heteromeric PC1/PC2 complex or acts as a chaperone to organize proteins in the endoplasmic reticulum for targeting to the plasma membrane (59). In this latter regard, the increased plasma protein expression and trafficking as observed by Groves et al. (60) may have in part functioned through its actions on the release of Gβγ dimers in the cell.

Thus, we postulate that GPSM1 associates with Gαi subunits leading to a redistribution of GPSM1 from its native cytoplasmic state to the plasma membrane (23). GPSM1 would then be in closer proximity to cell-surface proteins, such as GPCRs, to form Gαi-dependent multiprotein complexes, even in the presence of PTX (61). The inability to dissociate Gαi from the Gβγ subunits enables GPSM1 to maintain its interaction with these cell-surface GPCR–Gαi complexes (61). This would confirm our experiments that GPSM1 can act as a positive activator on PC1/PC2 channels by promoting Gβγ activity with or without PTX treatment (Fig. 5 and Fig. S4).

Under basal conditions where the GPSM1 expression in renal epithelial cells is virtually undetectable, we would anticipate that the cycling Gαi would be favored to associate with its cognate binding partner, Gβγ, and have a minimal role in modulating the PC1/PC2 ion channels. On the other hand, when GPSM1 expression is induced following biological insults or genetic damage, such as following ischemia-reperfusion injury or PKD (23, 24), there would be increased competition for the binding of Gαi-GDP between the GPR motifs in GPSM1 and other Gα-interacting proteins, resulting in a larger pool of free Gβγ. This would conceivably reduce the availability of intact heterotrimeric Gαβγ complexes and limit the extent of GPCR-mediated signaling (51, 62). Because of the diversity of function by GPSM1, there may be a context-dependent role for this protein in epithelial cell repair. In the absence of other genetic defects, biological injury to the renal epithelial cells would induce the expression of GPSM1 to promote accelerated epithelial cell recovery through Gβγ-mediated signal transduction events. In cystic epithelial cells, the increased levels of GPSM1 may act to partially compensate for reduced PC1/PC2 function, such that the cystic disease progression is blunted. Thus, the genetic ablation of GPSM1 leads to increased epithelial cell proliferation and accelerated cystic disease.

In conclusion, our genetic evidence sheds light on the mechanistic importance of accessory proteins and their associated heterotrimeric G proteins to control the dynamics of cystic disease progression through the modulation of polycystin function in renal epithelial cells. These data open the door for the development of drug therapies targeting GPSM1 and its associated downstream pathways to modulate cystic disease progression in PKD.

Materials and Methods

Mouse Strains and Breeding. Details on the animal breeding and genotyping are available in *SI Material and Methods* (25, 63).

Biological Measurements and Tissue Morphometry. Plasma, cyst fluid, and kidneys were isolated from mice at postnatal days 11–12 and 19, and these biological samples were processed as described in *SI Material and Methods*.

GPSM1 Immunoblot Analysis. The right kidneys were removed and immediately frozen on dry ice to measure the GPSM1 expression by immunoblot analysis as previously described by our laboratory (23, 24).

Renal Immunohistochemistry. Serial sections (4-μm thick) were stained with tubule segment-specific markers, Trichrome, or primary antibodies as described in *SI Material and Methods*.

Electrophysiological Measurements of PC1/PC2 Ion Channels. Reconstituted PC1/PC2 channel activity in the presence or absence of GPSM1 expression was measured in CHO cells as described in *SI Material and Methods* (34, 35).

Statistical Analysis. Data are expressed as mean ± SEM. All statistical analyses were performed using Prism 5.0 software (SAS Institute Inc.) as described in *SI Material and Methods*.

ACKNOWLEDGMENTS. The authors thank Dr. Stephen M. Lanier for the generation of the *Gpsm1*$^{-/-}$ mice with support from Grants NS24821 (to S.M.L.), DA025896 (to S.M.L.), and MH65092 (to J.B.B.) from the National Institutes of Health (NIH); the Physiology Biochemical Core at the Medical College of Wisconsin for biological fluid analysis; the National Institute of Diabetes and Digestive and Kidney Diseases-sponsored Johns Hopkins Polycystic Kidney Disease Research and Clinical Core Center (P30 DK090868) for *Pkd1*$^{V/+}$ mice and plasmids; and the NIH O'Brien Center for Acute Kidney Injury Research (P30 DK079337) for plasma creatinine measurements. Funding for this study was from NIH Grant DK090123 (to F.P.); Pilot and Feasibility funds

(to F.P.) from the Renal Center of Excellence in Pediatric Nephrology (Grant DK079306 to E.D.A.); institutional funds (to F.P.); interim support funds and NIH Grants GM086510 (to J.B.B.), HL108880 (to A.S.), and DK062199 (to F.Q.); and American Diabetes Association Grant 1-10-BS-168 (to A.S.).

1. The International Polycystic Kidney Disease Consortium (1995) Polycystic kidney disease: The complete structure of the PKD1 gene and its protein. *Cell* 81(2):289–298.
2. Hughes J, et al. (1995) The polycystic kidney disease 1 (PKD1) gene encodes a novel protein with multiple cell recognition domains. *Nat Genet* 10(2):151–160.
3. Mochizuki T, et al. (1996) PKD2, a gene for polycystic kidney disease that encodes an integral membrane protein. *Science* 272(5266):1339–1342.
4. Nadasdy T, et al. (1995) Proliferative activity of cyst epithelium in human renal cystic diseases. *J Am Soc Nephrol* 5(7):1462–1468.
5. Torres VE, Harris PC (2009) Autosomal dominant polycystic kidney disease: The last 3 years. *Kidney Int* 76(2):149–168.
6. Wilson PD (1997) Epithelial cell polarity and disease. *Am J Physiol* 272(4 Pt 2): F434–F442.
7. Qian F, et al. (1997) PKD1 interacts with PKD2 through a probable coiled-coil domain. *Nat Genet* 16(2):179–183.
8. Tsiokas L, Kim E, Arnould T, Sukhatme VP, Walz G (1997) Homo- and heterodimeric interactions between the gene products of PKD1 and PKD2. *Proc Natl Acad Sci USA* 94(13):6965–6970.
9. Boca M, et al. (2006) Polycystin-1 induces resistance to apoptosis through the phosphatidylinositol 3-kinase/Akt signaling pathway. *J Am Soc Nephrol* 17(3):637–647.
10. Delmas P, et al. (2004) Gating of the polycystin ion channel signaling complex in neurons and kidney cells. *FASEB J* 18(6):740–742.
11. Delmas P, et al. (2002) Constitutive activation of G-proteins by polycystin-1 is antagonized by polycystin-2. *J Biol Chem* 277(13):11276–11283.
12. Parnell SC, et al. (1998) The polycystic kidney disease-1 protein, polycystin-1, binds and activates heterotrimeric G-proteins in vitro. *Biochem Biophys Res Commun* 251(2): 625–631.
13. Parnell SC, et al. (2002) Polycystin-1 activation of c-Jun N-terminal kinase and AP-1 is mediated by heterotrimeric G proteins. *J Biol Chem* 277(22):19566–19572.
14. AbouAlaiwi WA, et al. (2009) Ciliary polycystin-2 is a mechanosensitive calcium channel involved in nitric oxide signaling cascades. *Circ Res* 104(7):860–869.
15. Blumer JB, Cismowski MJ, Sato M, Lanier SM (2005) AGS proteins: Receptor-independent activators of G-protein signaling. *Trends Pharmacol Sci* 26(9):470–476.
16. Blumer JB, Smrcka AV, Lanier SM (2007) Mechanistic pathways and biological roles for receptor-independent activators of G-protein signaling. *Pharmacol Ther* 113(3): 488–506.
17. Cismowski MJ, et al. (1999) Genetic screens in yeast to identify mammalian nonreceptor modulators of G-protein signaling. *Nat Biotechnol* 17(9):878–883.
18. Takesono A, et al. (1999) Receptor-independent activators of heterotrimeric G-protein signaling pathways. *J Biol Chem* 274(47):33202–33205.
19. Siderovski DP, Diversé-Pierluissi M, De Vries L (1999) The GoLoco motif: A Galphai/o binding motif and potential guanine-nucleotide exchange factor. *Trends Biochem Sci* 24(9):340–341.
20. Bernard ML, Peterson YK, Chung P, Jourdan J, Lanier SM (2001) Selective interaction of AGS3 with G-proteins and the influence of AGS3 on the activation state of G-proteins. *J Biol Chem* 276(2):1585–1593.
21. Sato M, Blumer JB, Simon V, Lanier SM (2006) Accessory proteins for G proteins: Partners in signaling. *Annu Rev Pharmacol Toxicol* 46:151–187.
22. Siderovski DP, Willard FS (2005) The GAPs, GEFs, and GDIs of heterotrimeric G-protein alpha subunits. *Int J Biol Sci* 1(2):51–66.
23. Nadella R, et al. (2010) Activator of G protein signaling 3 promotes epithelial cell proliferation in PKD. *J Am Soc Nephrol* 21(8):1275–1280.
24. Regner KR, et al. (2011) Loss of activator of G-protein signaling 3 impairs renal tubular regeneration following acute kidney injury in rodents. *FASEB J* 25(6):1844–1855.
25. Yu S, et al. (2007) Essential role of cleavage of Polycystin-1 at G protein-coupled receptor proteolytic site for kidney tubular structure. *Proc Natl Acad Sci USA* 104(47): 18688–18693.
26. Lantinga-van Leeuwen IS, et al. (2004) Lowering of Pkd1 expression is sufficient to cause polycystic kidney disease. *Hum Mol Genet* 13(24):3069–3077.
27. Blumer JB, Chandler LJ, Lanier SM (2002) Expression analysis and subcellular distribution of the two G-protein regulators AGS3 and LGN indicate distinct functionality. Localization of LGN to the midbody during cytokinesis. *J Biol Chem* 277(18): 15897–15903.
28. De Vries L, et al. (2000) Activator of G protein signaling 3 is a guanine dissociation inhibitor for Galpha i subunits. *Proc Natl Acad Sci USA* 97(26):14364–14369.
29. Sans N, et al. (2005) mPins modulates PSD-95 and SAP102 trafficking and influences NMDA receptor surface expression. *Nat Cell Biol* 7(12):1179–1190.
30. Geng L, Burrow CR, Li HP, Wilson PD (2000) Modification of the composition of polycystin-1 multiprotein complexes by calcium and tyrosine phosphorylation. *Biochim Biophys Acta* 1535(1):21–35.
31. Nauli SM, et al. (2003) Polycystins 1 and 2 mediate mechanosensation in the primary cilium of kidney cells. *Nat Genet* 33(2):129–137.
32. Newby LJ, et al. (2002) Identification, characterization, and localization of a novel kidney polycystin-1-polycystin-2 complex. *J Biol Chem* 277(23):20763–20773.
33. Tsiokas L, et al. (1999) Specific association of the gene product of PKD2 with the TRPC1 channel. *Proc Natl Acad Sci USA* 96(7):3934–3939.
34. Babich V, et al. (2004) The N-terminal extracellular domain is required for polycystin-1-dependent channel activity. *J Biol Chem* 279(24):25582–25589.
35. Hanaoka K, et al. (2000) Co-assembly of polycystin-1 and -2 produces unique cation-permeable currents. *Nature* 408(6815):990–994.
36. Oner SS, et al. (2010) Regulation of the AGS3·Galphai signaling complex by a seven-transmembrane span receptor. *J Biol Chem* 285(44):33949–33958.
37. Blumer JB, Oner SS, Lanier SM (2012) Group II activators of G-protein signalling and proteins containing a G-protein regulatory motif. *Acta Physiol (Oxf)* 204(2):202–218.
38. Kimple AJ, Bosch DE, Giguère PM, Siderovski DP (2011) Regulators of G-protein signaling and their Gα substrates: Promises and challenges in their use as drug discovery targets. *Pharmacol Rev* 63(3):728–749.
39. Weimbs T (2007) Polycystic kidney disease and renal injury repair: Common pathways, fluid flow, and the function of polycystin-1. *Am J Physiol Renal Physiol* 293(5): F1423–F1432.
40. Weimbs T (2011) Third-hit signaling in renal cyst formation. *J Am Soc Nephrol* 22(5): 793–795.
41. Bonventre JV (2003) Dedifferentiation and proliferation of surviving epithelial cells in acute renal failure. *J Am Soc Nephrol* 14(Suppl 1):S55–S61.
42. Bonventre JV, Weinberg JM (2003) Recent advances in the pathophysiology of ischemic acute renal failure. *J Am Soc Nephrol* 14(8):2199–2210.
43. Prasad S, McDaid JP, Tam FW, Haylor JL, Ong AC (2009) Pkd2 dosage influences cellular repair responses following ischemia-reperfusion injury. *Am J Pathol* 175(4): 1493–1503.
44. Zhao Y, Haylor JL, Ong AC (2002) Polycystin-2 expression is increased following experimental ischaemic renal injury. *Nephrol Dial Transplant* 17(12):2138–2144.
45. Happé H, et al. (2009) Toxic tubular injury in kidneys from Pkd1-deletion mice accelerates cystogenesis accompanied by dysregulated planar cell polarity and canonical Wnt signaling pathways. *Hum Mol Genet* 18(14):2532–2542.
46. Takakura A, Contrino L, Beck AW, Zhou J (2008) Pkd1 inactivation induced in adulthood produces focal cystic disease. *J Am Soc Nephrol* 19(12):2351–2363.
47. Takakura A, et al. (2009) Renal injury is a third hit promoting rapid development of adult polycystic kidney disease. *Hum Mol Genet* 18(14):2523–2531.
48. Peterson YK, et al. (2000) Stabilization of the GDP-bound conformation of Gialpha by a peptide derived from the G-protein regulatory motif of AGS3. *J Biol Chem* 275(43): 33193–33196.
49. Adhikari A, Sprang SR (2003) Thermodynamic characterization of the binding of activator of G protein signaling 3 (AGS3) and peptides derived from AGS3 with G alpha i1. *J Biol Chem* 278(51):51825–51832.
50. Fan P, Jiang Z, Diamond I, Yao L (2009) Up-regulation of AGS3 during morphine withdrawal promotes cAMP superactivation via adenylyl cyclase 5 and 7 in rat nucleus accumbens/striatal neurons. *Mol Pharmacol* 76(3):526–533.
51. Sato M, Gettys TW, Lanier SM (2004) AGS3 and signal integration by Galpha(s)- and Galpha(i)-coupled receptors: AGS3 blocks the sensitization of adenylyl cyclase following prolonged stimulation of a Galpha(i)-coupled receptor by influencing processing of Galpha(i). *J Biol Chem* 279(14):13375–13382.
52. Ghosh M, Peterson YK, Lanier SM, Smrcka AV (2003) Receptor- and nucleotide exchange-independent mechanisms for promoting G protein subunit dissociation. *J Biol Chem* 278(37):34747–34750.
53. Bowers MS, et al. (2008) Nucleus accumbens AGS3 expression drives ethanol seeking through G betagamma. *Proc Natl Acad Sci USA* 105(34):12533–12538.
54. Sanada K, Tsai LH (2005) G protein betagamma subunits and AGS3 control spindle orientation and asymmetric cell fate of cerebral cortical progenitors. *Cell* 122(1): 119–131.
55. Schwindinger WF, Robishaw JD (2001) Heterotrimeric G-protein betagamma-dimers in growth and differentiation. *Oncogene* 20(13):1653–1660.
56. Tian W, Zhang Z, Cohen DM (2000) MAPK signaling and the kidney. *Am J Physiol Renal Physiol* 279(4):F593–F604.
57. Tsiokas L, Kim S, Ong EC (2007) Cell biology of polycystin-2. *Cell Signal* 19(3):444–453.
58. Venkatachalam K, Montell C (2007) TRP channels. *Annu Rev Biochem* 76:387–417.
59. Dupré DJ, Robitaille M, Rebois RV, Hébert TE (2009) The role of Gbetagamma subunits in the organization, assembly, and function of GPCR signaling complexes. *Annu Rev Pharmacol Toxicol* 49:31–56.
60. Groves B, et al. (2007) A specific role of AGS3 in the surface expression of plasma membrane proteins. *Proc Natl Acad Sci USA* 104(46):18103–18108.
61. Casey PJ, Graziano MP, Gilman AG (1989) G protein beta gamma subunits from bovine brain and retina: Equivalent catalytic support of ADP-ribosylation of alpha subunits by pertussis toxin but differential interactions with Gs alpha. *Biochemistry* 28(2):611–616.
62. Oxford GS, Webb CK (2004) GoLoco motif peptides as probes of Galpha subunit specificity in coupling of G-protein-coupled receptors to ion channels. *Methods Enzymol* 390:437–450.
63. Blumer JB, et al. (2008) Activator of G protein signaling 3 null mice: I. Unexpected alterations in metabolic and cardiovascular function. *Endocrinology* 149(8):3842–3849.